Stability of the Earth Radiation Budget Experiment Scanner Results for the First Two Years of Multiple-Satellite Operation

W. FRANK STAYLOR

Atmospheric Sciences Division, NASA/Langley Research Center, Hampton, Virginia

(Manuscript received 6 October 1992, in final form 15 April 1993)

ABSTRACT

Clear-sky albedos and outgoing longwave radiation (OLR) determined from Earth Radiation Budget Experiment (ERBE) scanners on board the earth radiation budget satellite and *NOAA-9* spacecraft were analyzed for three target sites for the months February 1985–January 1987. The targets were oceans, deserts, and a multiscene site covering half the earth's surface. Year-to-year ratios of the monthly albedos and OLR were within the 0.98 –1.02 range with a standard error of about 1%. The data indicate that ERBE scanner measurements were stable to within a few tenths of a percent for the two-year period.

1. Introduction

The goal of the Earth Radiation Budget Experiment (ERBE) is to provide a dataset to study the regional, zonal, and global radiation properties of the earth at daily, monthly, seasonal, and annual time scales (Barkstrom et al. 1989). This radiation dataset must be highly accurate in order to detect and understand the often small, yet important global climate changes. To meet the stringent accuracy goals set for ERBE, the satellite orbits had to permit frequent coverage of the entire globe and the instruments had to provide high radiometric accuracy. Coverage errors are basically fixed by the number of satellites and their orbits (Harrison et al. 1983), while radiometric errors are determined by the design of the sensors and the degree to which their calibrations are known in flight. All of the ERBE instruments were extensively calibrated and characterized in a ground test facility; nonetheless, onboard calibration systems were provided to recalibrate the sensors and to validate their long-term stability in flight. A description of the ERBE sensors and their ground and onboard calibration systems is given by Barkstrom (1984).

In the early 1960s, radiometers exposed to the harsh space environment often degraded at alarming rates and the need for in-flight calibration became apparent. Consequently, onboard calibration systems were sometimes added that generally took the form of solar diffuser plates, incandescent lamps, or both, for shortwave channels and temperature-controlled blackbodies for longwave channels (Williamson 1977). Unfortunately, in-flight calibration systems can also fail, degrade, or become unusable for numerous reasons. Furthermore, their applicability is often questionable as they are usually activated in special calibration sequences (as were the ERBE scanners) that are substantially different from their earth viewing modes. Consequently, Staylor (1986) selected several desert sites that were to be used as natural earth targets to provide an additional check on the stability of the ERBE scanners and to allow a comparison of the *Nimbus-7* and ERBE scanner results. Earth targets have also been used by Jacobowitz et al. (1984), Whitlock et al. (1990), Brest and Rossow (1990), and Staylor (1990) to evaluate the stability of several scanners.

The use of earth targets inherently assumes that the targets will reflect (shortwave) or emit (longwave) predictable quantities of radiation. Stable surfaces such as deserts and oceans observed under similar solar and meteorological conditions at some later time should produce similar radiations. The present paper examines the stability of the albedo (ratio of reflected to incident shortwave radiation) and OLR (outgoing longwave radiation) results for several earth targets during the two-year period from February 1985 through January 1987, a period when both the earth radiation budget satellite (ERBS) and the *NOAA-9* ERBE scanners were operational. ERBE shortwave and longwave scanner stabilities will be assessed from comparisons of monthly averaged, clear-sky target albedos and OLR with those for the same month the following year when similar solar and meteorological conditions exist.

2. Satellite measurements

a. Instruments

Identical ERBE scanner instrument packages were flown on the ERBS, *NOAA-9*, and *NOAA-10* spacecraft.

Corresponding author address: W. F. Staylor, NASA/Langley Research Center, Mail Stop 420, Hampton, VA 23665-5225.

Each of the ERBE scanners had three broadband channels with thermistor bolometer detectors that measured reflected shortwave (0.2–5 μm), emitted longwave (5–50 μm), and total (0.2–>50 μm) radiances with a nadir ground resolution of about 40 km. The instruments scanned from horizon-to-horizon in 4 s using a view of space as a zero-radiance reference clamp. Normally, the instruments were scanned in a cross-track mode for global coverage, but infrequently were slewed 90° to scan along track to obtain data for modeling purposes. Each of the ERBE scanners had three onboard calibration systems—the internal calibration module (ICM), shortwave internal calibration source (SWICS), and the mirror attenuator mosaic (MAM). The ICM provided an electrically heated blackbody for calibration of the longwave and total channels. SWICS had a three-level tungsten lamp used for calibrating the shortwave channel, and the MAM was basically a solar reflector device that was used for shortwave and total channel calibrations. A more complete description of the ERBE scanners and their onboard calibration systems is given by Kopia (1986).

The ERBS scanner obtained useful radiance data from November 1984 until its failure in February 1990, the *NOAA-9* scanner from January 1985 to January 1987, and the *NOAA-10* scanner from November 1986 to May 1989. The present paper is based on scanner data taken from the ERBS and *NOAA-9* spacecraft for the two-year period from February 1985 through January 1987. January 1985 ERBS and *NOAA-9* data were eliminated because both spacecraft scanners were in along-track scanning modes for a substantial number of days during the month. The *NOAA-10* data were eliminated altogether because they provided only three months of overlap data with ERBS and *NOAA-9* during the two-year period of interest.

b. Orbits

The ERBS spacecraft was launched 5 October 1984 into a 600-km altitude orbit with an inclination of 57°. ERBS is in a precessing orbit with a repeat cycle of 72.8 days, meaning that it observes a given location an average of 20 min earlier each day. The *NOAA-9* spacecraft was launched 12 December 1984, into an 850-km orbit with an inclination of 99°. This was basically a sun-synchronous orbit with an initial ascending equatorial crossing time of 1430; however, the *NOAA-9* spacecraft precessed an average of 20 min later per year during the two-year period of interest here.

From the equator to about 30° latitude, both the ERBS and *NOAA-9* scanners observe all regions twice per day, once during daylight and once during nighttime hours. Above 30°, ERBS daily observations of a region increase substantially up to about 70° latitude, where useful ERBS measurements end. *NOAA-9* also obtains increased daily observations beginning at about 50° latitude, reaching a maximum of 14 times per day at the poles (i.e., once per orbit).

c. Albedo and OLR estimates

Six sequential steps are involved in the conversion of the basic scanner shortwave measurements into albedos: 1) Earth-reflected shortwave energy is absorbed by the thermistor bolometer chip producing a voltage that is converted to counts and transmitted to a ground center. There, the zero-radiance counts are subtracted and the difference is multiplied by a gain producing a filtered radiance, so denoted because the optical transmissions of the scanner telescopes are not unity nor spectrally flat. 2) Filtered radiances are converted to unfiltered radiances (i.e., unity shortwave spectral transmission) using the modeling work of Avis et al. (1984), which is a function of solar and viewing zenith angles, azimuth angle, and the viewed scene type (clear, overcast; ocean, land; etc.). 3) Unfiltered radiances are converted into albedos using angular direction models (Suttles et al. 1988) that are also functions of the same parameters given in (2). 4) ERBE divides the earth into 10 368 regions, each covering a 2.5° latitude $\times$ 2.5° longitude area. The 10–120 scanner measurements obtained from a region during each satellite overpass are first converted to albedos (steps 1–3) and then averaged to produce a regional albedo for the mean time of the overpass. 5) The 2–14 regional albedos obtained each day are converted into a daily albedo using diurnal models developed by Brooks et al. (1986). 6) Daily albedos for each day of a month are averaged to produce a monthly albedo for whatever sky conditions existed for that region. Steps 1–6 are also performed for the edited cloud-free scenes providing a clear-sky monthly albedo.

Steps involved in the conversion of the basic scanner longwave measurements into OLR are very similar to those for the shortwave. The major exceptions are that the unfiltering model for longwave radiances (Avis et al. 1984) is only a function of viewing zenith angle and scene type, and unfiltered radiances are converted into OLR using limb-darkening models (Suttles et al. 1989). All of the procedures (including the detector gains) involved in the estimation of the albedos and OLR as detailed above remained fixed during the two-year period of interest here.

Clear-sky albedos increase and OLR decrease with solar zenith angle, and, therefore, one should expect that monthly values would have annual cycles that respond to the varying solar conditions. However, barring substantial changes in the surface, atmosphere, or detector gain, one should expect a good comparison between site albedos or OLR with those for the same month in previous or following years (hereafter referred to as year-to-year comparisons) when solar conditions are identical. An examination of the estimation procedures suggests that only step 5 might produce differ-

cnccs that do not actually exist for the year-to-year comparisons. This could occur if the sampling times of the instantaneous measurements were substantially different from year to year and were input into diurnal models that were not error-free.

d. Sampling time

The ERBS spacecraft precesses about 20 min per day or 10 h per month. Averaged with the relatively constant *NOAA-9* sampling time, the mean sampling time for the ERBS–*NOAA-9* combination changes about 5 h per month. However, ERBS precessed five complete cycles in 364.1 days, and during the remaining 0.9 day of the year, precessed to about an 18-min-earlier sampling time. As stated previously, *NOAA-9* precessed an average of 20 min later per year. Hence, the mean ERBS–*NOAA-9* sampling time for a given day or month in 1985 was only 1 min different for the same day or month in 1986. This fortunate orbital timing virtually eliminates diurnal modeling as a source of any differences that might occur for year-to-year comparisons.

3. Sites

The present search for desirable target sites relied on previous works by Staylor (1986, 1990). Staylor found that desirable properties of a site included: 1) long-term stability, 2) high albedos and OLR combined with low solar zenith angles, 3) uniformity, 4) low cloudiness, and 5) sufficient size. One of the "sites" chosen by Staylor (1990) included all latitudinal zones from 30°N to 30°S, which covered half the earth's surface (3456 ERBE regions) and will hereafter be referred to as the 30°N–30°S site. Shown in Fig. 1, this site contains large areas of all major scene types (oceans, vegetated land, deserts, tropical forest, etc.) except snow, which is restricted mostly to a few high-elevation regions in the Himalayan and Andes mountains. The 30° latitudinal boundaries for this site were specifically set to reduce the effects that interannual differences of snow coverage might have on albedo and OLR comparisons.

There was concern that if shortwave sensor degradations were detected from the 30°N–30°S site comparisons, it would not be possible to determine whether the sensor had degraded uniformly across its broadband or had degraded only in a portion of its response spectrum. This is because the 30°N–30°S site is "multicolored" containing "blue" ocean, "green" vegetation, and "red" desert areas. The selection of additional target sites that emphasize the shorter- or longer-wavelength extrema of the scanner shortwave response spectrum seemed appropriate.

Top-of-the-atmosphere (TOA), clear-sky spectral albedos for ocean and desert surfaces are given in Fig. 2 for typical surface, atmospheric, and solar conditions (Suttles 1981). The spectral albedo for oceans is higher at the shorter wavelengths and lower at the longer wavelengths. Deserts have the reverse spectral characteristics, meaning that oceans and deserts might provide the best spectral extrema sites.

Locations of the ocean and desert spectral sites are shown in Fig. 1. The ocean site is located in the Pacific Ocean and is bounded by 45°N–45°S and 180°–230°E. This site covers almost 10% of the earth's surface (720 ERBE regions), and its surface is about 99.9% water. The desert site is a composite of a mostly desert area located in the vast Sahara Desert (20°–30°N, 0°–30°E) and a desert–arid land area located in Australia (20°–30°S, 120°–150°E), and together they cover 1.3% of the earth's surface (96 ERBE regions). These two desert areas are equal in size (10° × 30°) and in distance from the equator, meaning that the composite desert site is "equatorially balanced" as are the 30°N–30°S and ocean sites. By compositing the albedos from the two desert areas, better temporal and solar sampling are acquired for the larger single site than would have been obtained for the two smaller sites separately.

4. Site albedos and OLR

Monthly, clear-sky, regional albedos and OLR were obtained from ERBE S-4 data tapes, which are available from the archive at the National Space Science Data Center. Albedos and OLR for each of the three sites

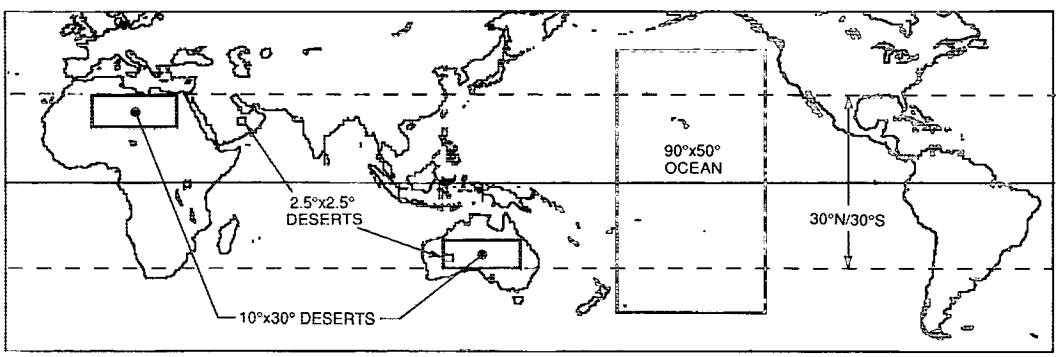

FIG. 1. Locations and boundaries of the 30°N–30°S, ocean, and desert sites.

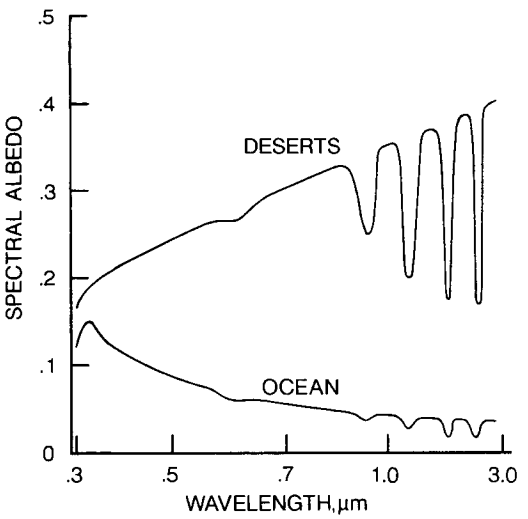

FIG. 2. TOA spectral albedos for oceans and deserts. Abscissa scale linear with cumulative spectral solar flux.

considered here are computed from the individual (96–3456) regional values that comprise the sites. Regional albedos (12–144) for each of the latitudinal zones (4–36) within a site were averaged and then weighted by the zonal areas and TOA solar fluxes. This procedure produced a true site albedo in that it is the ratio of the total shortwave energy that is reflected from the site to the total solar energy that falls on the site. Monthly OLR fluxes were obtained in a similar manner except they were not weighted by the TOA solar fluxes.

Monthly, clear-sky albedos for the 30°N–30°S, ocean, and desert sites for the 24 months from February 1985 through January 1987 are given in Table 1. Albedos for the first data year (February 1985–January 1986) are listed in the first column, the second data year (February 1986–January 1987) in the second column, and the ratio of the second-year albedos to the first-year albedos are listed in the third column for each of the three sites. All of the monthly, year-to-year albedo ratios are very near unity and range only from 0.98 to 1.02. The monthly site albedos are plotted in Fig. 3, and the 30°N–30°S and the ocean site are seen to exhibit dual annual cycles that peak at the solstices and valley at the equinoxes. Peaks occur when the site mean solar zenith angles are at maximum values, and valleys occur at minimum angles. The composite desert site exhibits only a single annual cycle primarily because the higher reflected fluxes from the brighter Sahara Desert overwhelm those from the darker Australian Desert in the composite albedo calculations.

Monthly, clear-sky OLR for the three sites are listed in Table 2 in the same format used for the albedos in Table 1. Similarly, all of the monthly, year-to-year OLR ratios are very near unity and range only from 0.99 to 1.01.

5. Albedo comparisons between satellites

Two desert sites were chosen by Staylor (1986) to serve as in-flight validation targets. The sites were 2.5° × 2.5° ERBE regions located in the bright Saudi Desert (20.0°–22.5°N, 50.0°–52.5°E; ERBE region number 3909) and in the dark Gibson Desert (25.0°–27.5°S, 120.0°–122.5°E; ERBE region number 6673) as shown in Fig. 1. *Nimbus-7* scanner data (taken in 1978 and 1979) were used to produce clear-sky, bidirectional reflectance models for each of the sites. The models express reflectance in terms of the solar and viewing zenith angles and were used to compute monthly albedos compatible with those from ERBE. Monthly albedos for the Saudi and Gibson deserts from ERBE (ERBS and *NOAA-9* combined) are compared to those from *Nimbus-7* in Fig. 4. The comparison is quite good as the mean values are virtually identical (ERBE 0.1% greater) and the standard deviation is only 3% of the mean value.

TABLE 1. Clear-sky site albedos, ERBS and *NOAA-9* combined.

	30°N–30°S			Ocean			Desert		
Month	First year	Second year	Second/first	First year	Second year	Second/first	First year	Second year	Second/first
February	0.1279	0.1259	0.9844	0.1093	0.1076	0.9844	0.2619	0.2611	0.9970
March	0.1270	0.1271	1.0008	0.1093	0.1092	0.9991	0.2641	0.2661	1.0076
April	0.1296	0.1282	0.9892	0.1079	0.1083	1.0037	0.2813	0.2785	0.9901
May	0.1329	0.1311	0.9865	0.1107	0.1092	0.9864	0.2858	0.2828	0.9895
June	0.1342	0.1348	1.0045	0.1107	0.1127	1.0181	0.2897	0.2898	1.0003
July	0.1328	0.1330	1.0015	0.1131	0.1126	0.9956	0.2856	0.2841	0.9947
August	0.1317	0.1308	0.9932	0.1106	0.1097	0.9919	0.2768	0.2777	1.0033
September	0.1285	0.1270	0.9883	0.1099	0.1077	0.9800	0.2679	0.2654	0.9907
October	0.1283	0.1267	0.9875	0.1094	0.1092	0.9982	0.2595	0.2571	0.9908
November	0.1278	0.1294	1.0125	0.1120	0.1130	1.0089	0.2520	0.2512	0.9968
December	0.1300	0.1308	1.0062	0.1127	0.1143	1.0142	0.2515	0.2510	0.9980
January	0.1320	0.1316	0.9970	0.1152	0.1140	0.9896	0.2561	0.2562	1.0004
Mean			0.9960			0.9975			0.9966
Standard deviation			0.0091			0.0120			0.0057

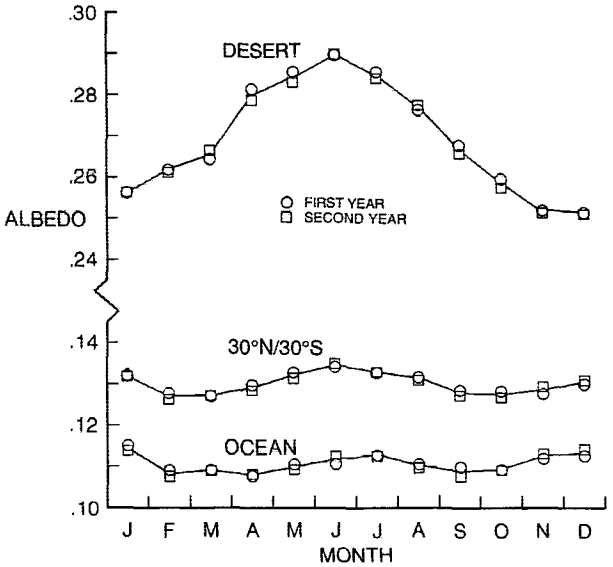

FIG. 3. Monthly, clear-sky site albedos.

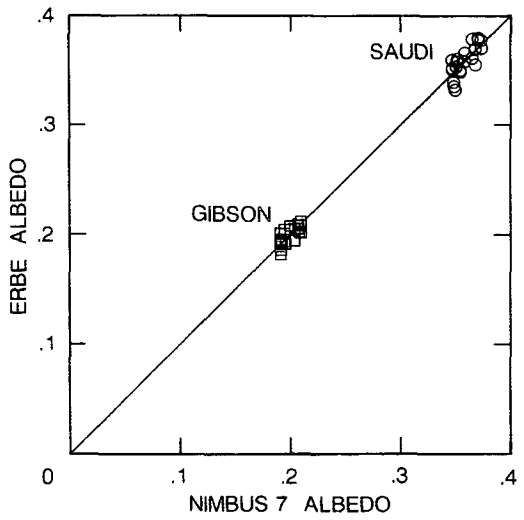

FIG. 4. Comparisons of the ERBE and *Nimbus-7* monthly, clear-sky albedos for the Gibson and Saudi deserts.

All of the ERBE albedos presented thus far were obtained from combined ERBS–*NOAA-9* measurements (see step 5). The ERBE S-4 data tapes also contain albedos computed separately for both the ERBS and *NOAA-9* spacecraft scanners. Monthly albedos for the Saudi and Gibson deserts from *NOAA-9* are compared to those obtained from ERBS in Fig. 5. Again, the comparison is quite good as the mean values are nearly identical (*NOAA-9* 0.4% greater) and the standard deviation is only 2% of the mean value.

6. Discussion of results

A basic assumption of the present work was that any changes in the monthly, year-to-year, clear-sky site albedos or OLR would reflect changes in the scanner sensor gains. This assumption was based on the fact that solar conditions, viewing angles, sampling times, computational procedures, etc. were identical for the same month the following year. At the bottoms of Tables 1 and 2, the mean and standard deviation of the monthly albedo and OLR ratios are given for each of the three sites, and the means ranged only from 0.994 to 0.999 and the deviations from 0.3% to 1.2%. The mean and standard deviation of the ratios for all 36 site-months combined is 0.9967 and 0.90%, respectively, for the albedo and 0.9968 and 0.47%, respectively, for the OLR. Lee and Barkstrom (1991) state that based on the in-flight ICS, SWICS, and MAM calibrations, the ERBE sensor gains were stable to about the 1% level for all channels.

TABLE 2. Clear-sky site OLR (W m^{-2}), ERBS and *NOAA-9* combined.

Month	30°N–30°S			Ocean			Desert		
	First year	Second year	Second/first	First year	Second year	Second/first	First year	Second year	Second/first
February	286.3	285.6	0.9975	280.0	281.5	1.0054	287.5	285.3	0.9923
March	287.4	287.9	1.0018	280.2	282.0	1.0065	287.4	286.8	0.9981
April	288.2	286.3	0.9935	279.9	279.3	0.9976	289.8	286.7	0.9893
May	288.6	286.7	0.9934	281.5	279.4	0.9923	288.2	286.1	0.9928
June	287.6	287.0	0.9981	281.3	281.9	1.0020	289.9	287.5	0.9915
July	286.2	286.3	1.0002	282.4	281.8	0.9980	292.2	290.5	0.9942
August	288.0	287.0	0.9966	285.1	282.9	0.9921	295.8	292.4	0.9885
September	287.7	286.6	0.9962	283.7	282.0	0.9941	293.9	290.3	0.9879
October	288.0	287.3	0.9975	283.0	282.9	0.9994	285.4	286.5	1.0040
November	287.0	287.1	1.0004	281.7	281.3	0.9987	284.8	285.7	1.0032
December	286.8	286.5	0.9991	281.8	282.4	1.0023	285.8	283.3	0.9914
January	288.1	287.4	0.9977	284.2	282.3	0.9933	285.1	284.2	0.9970
Mean			0.9977			0.9985			0.9942
Standard deviation			0.0026			0.0049			0.0054

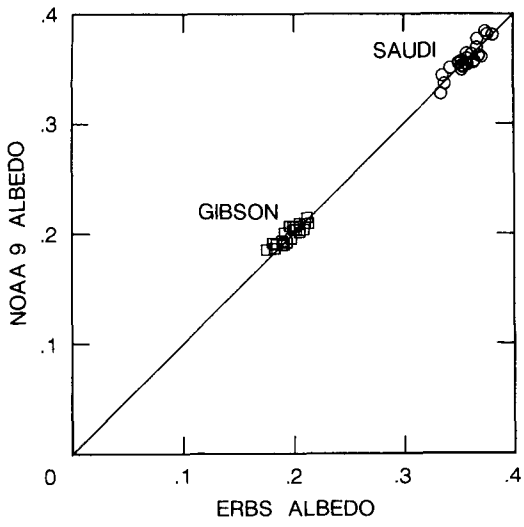

FIG. 5. Comparisons of *NOAA-9* and ERBS monthly, clear-sky albedos for the Gibson and Saudi deserts.

The author had no difficulty in detecting a 6% per year degradation for the visible channel of the Advanced Very High Resolution Radiometer that was also on board the *NOAA-9* spacecraft (Staylor 1990). However, the author now finds it difficult to conclude from the data here that any consistent degradation of the ERBS–*NOAA-9* scanner sensors occurred during the two-year period from February 1985 through January 1987. For instance, if only the last three comparison months were considered (November–January), one might conclude that the shortwave sensor gains had slightly increased (0.3%). Essentially the same results were obtained for all three ERBS–*NOAA-9* target sites suggesting that no spectral response shifts occurred during the period. The excellent comparisons of the ERBE and *Nimbus-7* and the *NOAA-9* and ERBS albedo results for bright and dark deserts provide positive ties between these datasets.

The albedo of the earth is about 0.3, and therefore, its global reflected flux averages about 100 W m^{-2}. If for the sake of argument it were assumed that the ERBE sensors degraded 0.3%, this would amount to a shortwave flux error of 0.3 W m^{-2} and a longwave flux error of 0.7 W m^{-2}. The accuracy goal set for ERBE prior to launch was 1 W m^{-2} (Barkstrom 1984).

7. Summary

Monthly, clear-sky albedos and OLR determined from ERBE scanners on board the ERBS and *NOAA-9* spacecraft were compared for three target sites for two years, February 1985–January 1987. The targets included a multicolored site (30°N–30°S) covering half the earth's surface, a blue ocean site (Pacific), and a composite red desert site (Sahara/Australia).

Monthly, year-to-year comparisons for all sites fell within the 0.98 to 1.02 ratio range for the albedos and within the 0.99 to 1.01 ratio range for the OLR with a standard deviation of about 1% for both. The data indicate that the ERBE albedos and OLR were stable to within a few tenths of a percent for the two-year period. For the Saudi and Gibson desert sites, plots of the ERBS–*NOAA-9* (combined) versus *Nimbus-7* albedos and the *NOAA-9* versus ERBS albedos showed agreement to within a few tenths of a percent.

REFERENCES

Avis, L. M., R. N. Green, J. T. Suttles, and S. K. Gupta, 1984: A robust pseudo-inverse spectral filter applied to the Earth Radiation Budget Experiment (ERBE) scanning channels. NASA TM 85781, 32 pp.

Barkstrom, B. R., 1984: The Earth Radiation Budget Experiment (ERBE). *Bull. Amer. Meteor. Soc.*, **65,** 1170–1185.

——, E. Harrison, G. Smith, R. Green, J. Kibler, R. Cess, and the ERBE Science Team, 1989: Earth Radiation Budget Experiment (ERBE) archival and April 1985 results. *Bull. Amer. Meteor. Soc.*, **70,** 1254–1262.

Brest, C. L., and W. B. Rossow, 1990: Radiometric calibration and monitoring of NOAA AVHRR data for ISCCP. *Int. J. Remote Sens.*, **13,** 235–274.

Brooks, D. R., E. F. Harrison, P. Minnis, J. T. Suttles, and R. S. Kandel, 1986: Development of algorithms for understanding the temporal and spatial variability of the earth's radiation balance. *Rev. Geophys.*, **24,** 422–438.

Harrison, E. F., P. Minnis, and G. G. Gibson, 1983: Orbital and cloud cover sampling analyses for multisatellite earth radiation budget experiments. *J. Spacecr. and Rockets,* **20,** 491–495.

Jacobowitz, H., H. V. Soule, H. L. Kyle, F. B. House, and the *Nimbus-7* ERB Experiment Team, 1984: The Earth Radiation Budget (ERB) Experiment: An overview. *J. Geophys. Res.*, **89,** 5021–5038.

Kopia, L. P., 1986: Earth Radiation Budget Experiment scanner instrument. *Rev. Geophys.*, **24,** 400–406.

Lee, R. B., III, and B. R. Barkstrom, 1991: Characterization of the Earth Radiation Budget Experiment radiometers. *Metrologia,* **28,** 183–187.

Staylor, W. F., 1986: Site selection and directional models of deserts used for ERBE validation targets. NASA TP 2540, 12 pp.

——, 1990: Degradation rates of the AVHRR visible channel for the NOAA 6, 7, and 9 spacecraft. *J. Atmos. Oceanic. Technol.*, **7,** 411–423.

Suttles, J. T., 1981: Anisotropy of solar radiation leaving the earth-atmosphere system. Ph.D. dissertation, Department of Mechanical Engineering, Old Dominion University, 180 pp.

——, R. N. Green, P. Minnis, G. L. Smith, W. F. Staylor, B. A. Wielicki, I. J. Walker, D. F. Young, V. R. Taylor, and L. L. Stowe, 1988: Angular radiation models for the earth–atmosphere system. Volume I—Shortwave radiation. NASA RP 1184, 144 pp.

——, ——, G. L. Smith, B. A. Wielicki, I. J. Walker, V. R. Taylor, and L. L. Stowe, 1989: Angular radiation models for earth–atmosphere system. Volume II—Longwave radiation. NASA RP 1184, 84 pp.

Whitlock, C. H., W. F. Staylor, J. T. Suttles, G. Smith, R. Levin, R. Frouin, C. Gautier, P. M. Teillet, P. N. Slater, Y. J. Kaufman, B. N. Holben, W. B. Rossow, C. L. Brest, and S. R. LeCroy, 1990: AVHRR and VISSIR instrument calibration results for both cirrus and marine stratocumulus IFO periods. NASA CP 3083, 141–144.

Williamson, L. E., Ed., 1977: *Calibration Technology for Meteorological Satellites.* First ed. *Atmos. Sci. Lab. Monogr.*, Ser. 3, U.S. Army, 139 pp. [Available from DTIC as AD A041 662.]